

Heart Remodelling Affects ECG in Rat DOCA/Salt Model

Michal LASKA¹, Jiri VITOUS², Radovan JIRIK², Michal HENDRYCH³, Eva DRAZANOVA^{2,4}, Lucie KRATKA², Jaroslav NADENICEK¹, Marie NOVAKOVA¹, Tibor STRACINA¹

¹Department of Physiology, Faculty of Medicine, Masaryk University, Brno, Czech Republic,

²Institute of Scientific Instruments, Czech Academy of Sciences, Brno, Czech Republic, ³First Department of Pathology, St. Anne's University Hospital Brno and Faculty of Medicine, Masaryk University, Brno, Czech Republic, ⁴Department of Pharmacology, Faculty of Medicine, Masaryk University, Brno, Czech Republic

Received July 9, 2024

Accepted October 24, 2024

Summary

Myocardial remodelling involves structural and functional changes in the heart, potentially leading to heart failure. The deoxycorticosterone acetate (DOCA)/salt model is a widely used experimental approach to study hypertension-induced cardiac remodelling. It allows to investigate the mechanisms underlying myocardial fibrosis and hypertrophy, which are key contributors to impaired cardiac function. In this study, myocardial remodelling in rat deoxycorticosterone acetate/salt model was examined over a three-week period. The experiment involved 11 male Sprague-Dawley rats, divided into two groups: fibrosis (n=6) and control (n=5). Myocardial remodelling was induced in the fibrosis group through unilateral nephrectomy, deoxycorticosterone acetate administration, and increased salt intake. The results revealed significant structural changes, including increased left ventricular wall thickness, myocardial fractional volume, and development of myocardial fibrosis. Despite these changes, left ventricular ejection fraction was preserved and even increased. ECG analysis showed significant prolongation of the PR interval and widening of the QRS complex in the fibrosis group, indicating disrupted atrioventricular and ventricular conduction, likely due to fibrosis and hypertrophy. Correlation analysis suggested a potential relationship between QRS duration and myocardial hypertrophy, although no significant correlations were found among other ECG parameters and structural changes detected by MRI. The study highlights the advantage of the DOCA/salt model in exploring the impact of myocardial remodelling on electrophysiological properties. Notably, this study is among the first to show that early myocardial remodelling in this model is accompanied by distinct electrophysiological changes, suggesting that advanced methods combined with

established animal models can open new opportunities for research in this field.

Key words

Myocardial fibrosis • Remodelling • Animal model • DOCA-salt • Magnetic resonance imaging

Corresponding author

T. Stracina, Department of Physiology, Faculty of Medicine, Masaryk University, Kamenice 5, 625 00 Brno, Czech Republic.
E-mail: stracina@med.muni.cz

Introduction

Hypertension is the leading risk factor for cardiovascular health, with its prevalence increasing globally, particularly due to the ageing of the population and unhealthy lifestyle [1]. Hypertension is characterized by abnormally high arterial blood pressure, defined in adults as a systolic blood pressure of 140 mm Hg or greater or a diastolic blood pressure of 90 mm Hg or greater [2]. Elevated blood pressure triggers pathophysiological processes that have systemic consequences, making hypertension a major risk factor for stroke, myocardial infarction, renal failure, and heart failure [3].

Among others, significant consequence of hypertension is myocardial remodelling. Initially, the heart adapts to the increased pressure load, maintaining mechanical function and adequate tissue oxygenation. However, this adaptation is followed by a remodelling process involving a range of subcellular, cellular, and

extracellular changes [4,5]. Although cardiac function may remain preserved for some time, persistent hypertension eventually leads to pathological remodelling, characterized by inadequate oxygen delivery and impaired cardiac function [5]. The mechanisms underlying myocardial remodelling include hypertrophy and fibrosis.

Myocardial fibrosis is characterized by excessive amount of extracellular matrix produced by activated fibroblasts. Patients with myocardial fibrosis face an increased risk of ventricular arrhythmias, sudden cardiac death, and heart failure [6]. The arrhythmogenic potential of remodelled myocardium indicates an occurrence of changes in electrophysiological characteristics of the heart tissue. While the relationship between fibrosis and arrhythmias is well established in clinical settings, there is limited evidence about the specific electrophysiological changes that occur in animal models of myocardial fibrosis.

Animal models still remain crucial for understanding the mechanisms of myocardial fibrosis. These models enable studying of complex pathophysiological processes at the cellular level and at the same time the consequences of heart remodelling from a macroscopic perspective. In this area of preclinical research, laboratory rats and mice are the most commonly used species.

According to Wang *et al.*, rodent models of myocardial fibrosis can be categorized into three groups [7]. The first group includes models primarily developed to study hypertension and hypertensive heart disease, including those with a genetic predisposition for hypertension, such as the frequently used spontaneously hypertensive rat model [8]. Other hypertension models involve administration of substances such as angiotensin II or nitroxide synthase inhibitors [9,10]. Hypertension can also be induced surgically, as in transverse aortic constriction model, which is typically performed in mice [7,11]. The second group uses myocardial ischemia to induce replacement fibrosis [7], which can be triggered by left coronary artery ligation [11] or by administering isoprenaline [12]. The third group comprises rodent models exposed to high sodium intake to develop reactive fibrosis. Among these models, the deoxycorticosterone acetate/salt (DOCA/salt) model is particularly reliable for inducing myocardial fibrosis [7].

The DOCA/salt model combines DOCA administration, high sodium intake, and unilateral

nephrectomy [13]. Fully developed model is characterized by pressure-volume overload, resulting in myocardial remodelling, including hypertrophy and fibrosis [13].

Over the past two decades, animal research has remarkably advanced. Technological breakthroughs have introduced more robust and sensitive measurement instruments tailored to small animal models. This in turn has facilitated the rapid processing of large datasets through enhanced computing power, machine learning algorithms, and artificial intelligence technologies. Engaging well-established animal models with these novel high-end techniques has the potential to unlock new avenues in biomedical research.

This study aims to identify ECG alterations in remodelled myocardium within the DOCA/salt rat model and to comprehensively elucidate correlations between these ECG changes and structural modifications. By investigating the intricate interplay among these parameters, the study aims to provide an insight into the complex dynamics characterizing cardiac remodelling in the DOCA/salt model.

Materials and Methods

Animal model

The animal experiment was carried out according to the recommendations of the European Community Guide for the Care and Use of Laboratory Animals and according to the experimental protocols (No. MSMT-35972/2020-3 and MSMT-2383/2023-5) approved by the Committee for Ensuring the Welfare of Laboratory Animals, Masaryk University and licensed by the Ministry of Education, Youth and Sports of the Czech Republic.

A total of 11 male Sprague-Dawley rats (6 weeks old) were included in the study. The animals were randomly divided into two groups: fibrosis (F; n=6; m=276.0±14.2 g) and controls (C; n=5; m=236.4±13.7 g). The animals were housed in groups in a temperature-, pressure-, and humidity-controlled environment, with 12/12 light/dark cycle. Water and standard diet were accessible *ad libitum* during the whole experiment. The animals were allowed to adapt to the environment and daily handling for a minimum of 7 days. The deoxycorticosterone acetate (DOCA; Sigma-Aldrich, USA) – salt model was used to induce myocardial fibrosis in the group F, as previously described [14]. Briefly, an unilateral nephrectomy was performed.

DOCA was administered once a week for three following weeks in the depot dose (20 mg/week, s.c.; dissolved in 0.2 ml of peanut oil). During the same period, salt intake was increased by adding sodium chloride and potassium chloride into the drinking water (0.9 % NaCl and 0.3 % KCl). In the control group (C), a sham operation was performed, and the animals received subcutaneous injections of the vehicle (0.2 ml peanut oil, Sigma-Aldrich, USA) once a week for three weeks, without the addition of salt to the drinking water. During the whole experiment, animals from both groups were regularly weighed.

ECG acquisition and analyses

At the end of the experiment, each rat was anaesthetized using ketamine/xylazine (90 mg/kg and 8 mg/kg, respectively; i.p.) and placed on the heated pad. In general anaesthesia, one bipolar lead of ECG was continually recorded for 15 min. ECG was recorded using needle electrodes, ECG Bio Amplifier and PowerLab acquisition hardware, and LabChart 8 Pro software (AD Instruments Ltd., CO, USA). The rectal temperature was measured alongside the ECG recording. ECG was analysed using ECG module in LabChart software. Five-minutes-long interval with regular cardiac rhythm was selected for analysis. ECG patterns were averaged and following parameters were evaluated: P wave duration, PR interval duration, QRS interval width, and QT interval duration. QT interval was corrected using Hodge's formula.

Magnetic resonance imaging

To analyse myocardial remodelling progress, *in vivo* magnetic resonance imaging (MRI) was performed at the Institute of Scientific Instruments, Czech Academy of Sciences, Brno (ISI) using a 9.4T magnetic-resonance scanner for small-animal examinations (Bruker BioSpin GmbH, Ettlingen, Germany). The first imaging session was performed before the induction of the DOCA/salt model. The repeated measurements were performed two and three weeks after model induction. ISI's retrospectively gated golden-angle T1-quantification acquisition was performed before (native) and after (postcontrast) i.v. administration of a contrast agent, as previously described [14]. In addition, cardiac anatomy was evaluated using Bruker's retrospectively gated multi-slice Inragate FLASH, and anatomical images were processed manually to assess endo- and epicardial contours of the left ventricle (LV). The following

anatomical parameters of the LV were assessed: LV wall thickness in systole (sLVW) and diastole (dLVW), systolic (sLVD) and diastolic diameter of the LV (dLVD), and myocardial fractional volume (MFV). Moreover, the left ventricular ejection fraction (LVEF) was estimated.

Histopathological quantification of myocardial fibrosis

To quantify myocardial fibrosis, histological analysis was performed. At the end of the experiment, the animals were sacrificed, and the hearts were excised. The entire hearts were fixed in formalin for 24 h and then sectioned into three slices: one at the basal part of the ventricles, second one at the level of the papillary muscles, and a third one at the apical part of the ventricles. The samples were routinely processed into formalin-fixed paraffin-embedded blocks and sliced into tissue sections. The sections were stained using haematoxylin-eosin. Myocardial fibrosis was manually annotated by an expert using QuPath software on whole-slide images [15]. The analysis was finalized by calculating the ratio of fibrotic areas to the total tissue area, expressed as a percentage.

Statistical analyses

Statistical analyses were performed using GraphPad Prism 10 (GraphPad Software, CA, USA). Data distribution was tested by the Shapiro-Wilk normality test. Because of normal Gaussian data distribution, parametric statistical analysis was employed. Unpaired *t*-test with Welch's correction was used to compare the two groups (F vs. C), and paired *t*-tests were used for paired measurements. Pearson correlation analysis was conducted to assess the relationships among MRI and ECG parameters. To provide a comprehensive understanding of the relationships between these parameters, correlations were calculated across all animals, irrespective of their assignment to experimental groups. Pearson correlation coefficients (*r*) were calculated to quantify the strength and direction of the linear relationships between the variables. The results are presented as mean \pm SD. *p*-values below 0.05 were considered statistically significant.

Results

Histological changes

Histopathological examination revealed significant development of interstitial, perivascular, and

replacement fibrosis in group F ($0.86 \pm 0.73\%$ of the tissue sample area affected by fibrosis; $p=0.0346$ compared to controls). Fibrosis was observed in both the left and right ventricular walls (Fig. 1). No myocardial fibrosis was detected in any of the samples from group C.

ECG parameters

Although P wave duration did not significantly differ between the groups ($p=0.1727$), the PR interval was significantly prolonged in the fibrotic hearts (F; 55.6 ± 4.5 ms) compared to controls (C; 43.0 ± 1.1 ms; $p=0.0333$; Fig. 2).

In group F, the QRS complex (19.6 ± 1.3 ms) was significantly wider than in group C (17.3 ± 1.5 ms; $p=0.0486$). The QTc interval showed insignificant prolongation in group F (525.9 ± 97.2 ms) as compared to group C (463.8 ± 22.0 ms; $p=0.1840$; Fig. 2).

Evaluation of Magnetic Resonance Imaging

Structural parameters of the left ventricle

Representative anatomical MRI images of the left ventricle from both the fibrosis and control groups are shown in Figure 3. In group F, both sLVW and dLVW significantly increased during the experiment. Systolic LVW increased from 3.50 ± 0.41 mm before to 4.49 ± 0.56 mm three weeks after the model induction ($p=0.0180$). Diastolic LVW increased from 1.75 ± 0.18 mm before to 2.70 ± 0.37 mm three weeks after the model induction ($p=0.0035$; Fig. 4). In group C, no significant change in sLVW and dLVW was observed. Before the model induction, no significant differences between the groups were detected in sLVW as well as in dLVW. At the end of the experiment, dLVW was significantly greater in group F compared to group C (2.70 ± 0.37 mm vs. 1.70 ± 0.14 mm; $p=0.0007$). However, the difference between the groups in sLVW was insignificant (group F: 4.49 ± 0.56 mm; group C: 3.56 ± 0.81 ; $p=0.0639$; Fig. 4).

No significant changes in systolic or diastolic LV diameters (sLVD, dLVD) were detected in either group during the experiment.

Myocardial fractional volume

Values of MFV are summarized in Table 1. There was no difference in MFV between the groups before the model induction. In group F, myocardial fractional volume (MFV) significantly increased two weeks ($p=0.0034$) and three weeks ($p=0.0013$) post-induction, indicating progressive myocardial remodelling.

In contrast, no significant changes were observed in group C throughout the experiment. In group F, MFV was significantly higher as compared to group C two weeks ($p=0.0477$) as well as three weeks after the model induction ($p=0.0011$).

The left ventricular ejection fraction

Values of LVEF are summarized in Table 1. In group F, LVEF was significantly increased in the second ($p=0.0412$) and the third week ($p=0.0391$) as compared to LVEF before the model induction. In group C, significant increase in LVEF was also detected in the third week ($p=0.0266$). Before the model induction, no significant LVEF difference between the groups was detected. Two weeks after the model induction, LVEF in group F was significantly higher than in group C ($p=0.0217$). At the end of the experiment, the difference between the groups was even more significant ($p=0.0020$).

Correlations

A positive correlation between QRS duration and MFV approached statistical significance ($r=0.6298$; $p=0.0510$), suggesting a trend towards a relationship between electrical conduction changes and myocardial remodelling. No correlations were detected between QRS and dLVW, QRS and sLVW, QTc and MFV, QTc and dLVW, as well as QTc and sLVW. Significant positive correlation was detected between myocardial fractional volume and the left ventricular ejection fraction ($r=0.6508$; $p=0.0301$).

Discussion

In this study, myocardial remodelling was successfully induced in the F group within three weeks following the model induction. The remodelling was triggered by pressure-volume overload, established through unilateral nephrectomy, DOCA administration, and salt supplementation in drinking water.

DOCA/salt: An animal model of hypertension

DOCA/salt model represents pharmacologically and renal-induced secondary hypertension [16]. The initial phase of the experiment involves a rise in blood pressure, driven by the combined effects of DOCA and saline. This is followed by the second phase characterized by sustained hypertension over several weeks [13].

Salt plays a critical role in this model by increasing the severity and accelerating the onset of

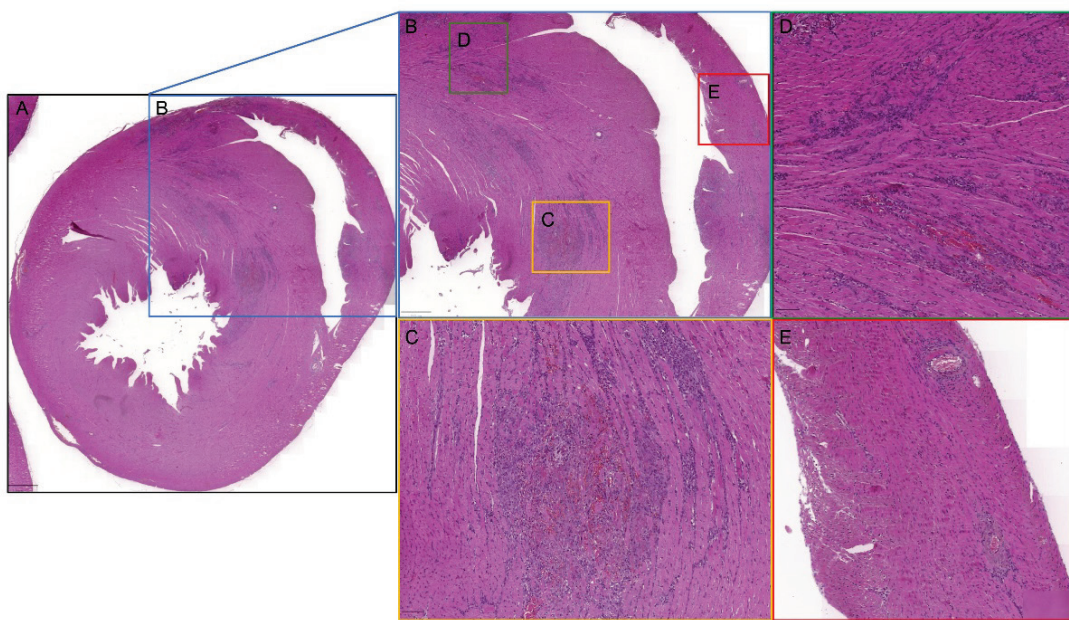


Fig. 1. Histological evaluation of myocardial fibrosis. **(A)** A whole slide scan of a cross-section of the heart. **(B)** An image zoomed in on the left and right ventricles. **(C)** Detailed images showing replacement fibrosis, **(D)** interstitial fibrosis in the left ventricle and **(E)** perivascular fibrosis in the right ventricle. Haematoxylin-eosin staining.

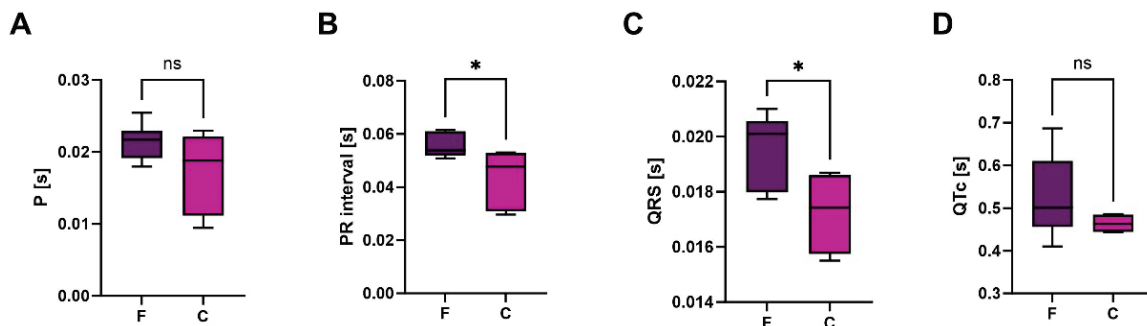


Fig. 2. Electrocardiographic parameters. **(A)** P wave duration. **(B)** PR interval duration. **(C)** QRS complex width. **(D)** QTc interval duration. The boxes represent the interquartile range, with the line inside the box indicating the median. Whiskers extend to the minimum and maximum values of the datasets. F – Animals with induced myocardial fibrosis (group F); C – control animals (group C); ns – no significant difference; * $p < 0.05$; ** $p < 0.01$; *** $p < 0.001$.

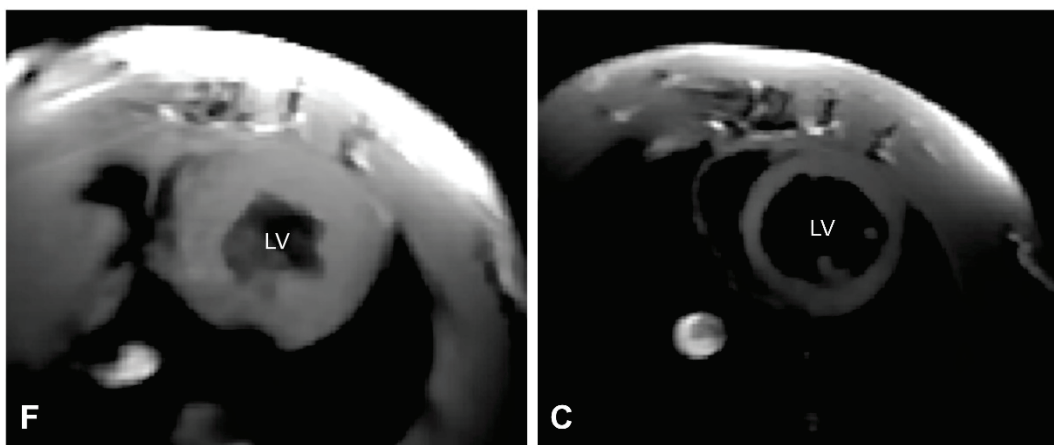


Fig. 3. Representative anatomical MRI images of the left ventricle. **(F)** Animal with induced myocardial fibrosis (group F); **(C)** control animal (group C). Images were acquired using Bruker's retrospectively gated multi-slice Intrigate FLASH technique. Endo- and epicardial contours of the left ventricle (LV) were manually delineated to assess structural changes. Group F shows increased LV wall thickness and myocardial fractional volume compared to the control group, consistent with myocardial remodelling.

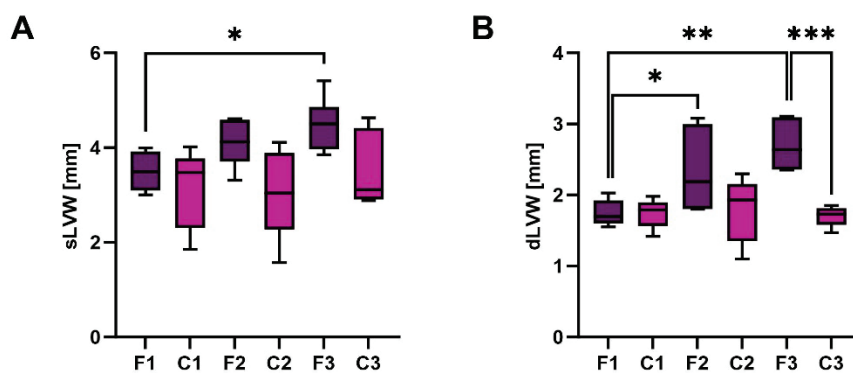


Fig. 4. The left ventricular wall thickness in systole and diastole. **(A)** Systolic left ventricular wall thickness (sLVW). **(B)** Diastolic left ventricular wall thickness (dLVW). The boxes represent the interquartile range, with the line inside the box indicating the median. Whiskers extend to the minimum and maximum values of the datasets. * $p < 0.05$; ** $p < 0.01$; *** $p < 0.001$.

Table 1. The left ventricular ejection fraction and myocardial fractional volume.

Week of the measurement	LVEF [%]		MFV [%]	
	Group F	Group C	Group F	Group C
0	78.09 ± 7.25	76.56 ± 4.47	58.49 ± 1.19	61.98 ± 5.50
2	$85.60 \pm 2.70^{*,\#}$	78.65 ± 4.50	$65.39 \pm 3.02^{**,\#}$	60.96 ± 3.26
3	$87.63 \pm 1.62^{**,\#}$	$82.86 \pm 1.87^*$	$70.86 \pm 4.64^{**,\#}$	59.60 ± 1.71

Data are presented as mean \pm SD. LVEF – left ventricular ejection fraction; MFV – myocardial fractional volume; 0 – before the model induction; 2 – two weeks after the model induction; 3 – three weeks after the model induction; * paired t -test (vs. week 0); $\#$ unpaired t -test (between the groups); */# $p < 0.05$; **/## $p < 0.01$.

hypertension. Besides the direct elevation of NaCl plasma levels *via* DOCA-induced sodium retention in the kidneys [16], salt also stimulates the sympathetic nervous system, contributing to the blood pressure rise. O'Donaughy *et al.* [17] demonstrated increased sympathetic activity in the lumbar region of DOCA/salt rats, suggesting that DOCA heightens the sympatho-excitatory response to elevated plasma NaCl levels. Even a slight increase in plasma NaCl concentration significantly elevates blood pressure. Additionally, increased blood osmolality stimulates osmoreceptors in the brain, thus further supporting the hypertension observed in this model [17].

Despite the known low plasma renin levels in the DOCA/salt model, the renin-angiotensin-aldosterone system (RAAS) is still activated, particularly in specific brain compartments. Elevated angiotensin II levels in brain nuclei influence blood pressure regulation by acting on AT1 receptors in critical areas [18].

DOCA/salt: An animal model of myocardial remodelling

The volume overload in our experiment, induced by DOCA's stimulation of mineralocorticoid receptors, led to sodium retention and water reabsorption in the

remaining kidney, creating hypervolemic conditions [13]. The resultant pressure-volume overload triggered cardiac hypertrophy, as evidenced by increased left ventricular wall thickness (LVW) and myocardial fractional volume (MFV). Over the course of three weeks, this remodelling progressed into a pathological phase, characterized by excessive collagen deposition [19] and the development of myocardial fibrosis, as confirmed by histological analysis. These findings align with those of Grobe *et al.* [20].

Despite the pathological remodelling, a decrease in left ventricular ejection fraction (LVEF) was not observed in our study. In fact, LVEF, a key indicator of ventricular contractility, increased in the F group. This is consistent with the findings of Brown *et al.*, who reported preserved ventricular contractility up to the fourth week in a similar experiment, with decreased LVEF only manifesting after the eighth week [19]. Wang *et al.* classified the DOCA/salt model as the one of heart failure with preserved ejection fraction and diastolic dysfunction [7], which is consistent with our findings – we observed increased LV ejection fraction and increased diastolic LV wall thickness. The positive correlation between LVEF and MFV suggests that preserved (and even

increased) ejection fraction is linked to myocardial hypertrophy. However, the increased diastolic LV wall thickness points to diastolic dysfunction, characterized by impaired cardiomyocyte relaxation. Lovelock *et al.* proposed that this diastolic dysfunction might be driven by oxidative stress on the contractile apparatus [21]. Oxidative stress appears to be a key factor in the transition from adaptive (physiological) hypertrophy to maladaptive (pathological) hypertrophy [6].

DOCA/salt: A model of electrophysiological remodelling

ECG alterations in our study indirectly reflect myocardial remodelling. Structural, metabolic, and biochemical changes in the heart during remodelling modify intracellular processes and ion homeostasis [22]. In the F group, we observed prolongation of the PR interval, indicating altered impulse propagation at the atrioventricular level, and widening of the QRS complex, reflecting disrupted ventricular conduction. Action potential propagation is impaired by fibrotic tissue, which is electrically inert [23]. Hypertrophy also contributes to electrophysiological alterations. As reported by Momtaz *et al.*, severe hypertrophy is associated with a significant reduction in transient outward potassium current density, which is crucial for cardiomyocyte repolarization and action potential duration [24]. Moreover, hypertrophy in the DOCA/salt model downregulates certain genes encoding left ventricular potassium channels, further prolonging the action potential [25]. Coulombe *et al.* reported increased duration of plateau in hypertrophic hearts, further complicating the electrophysiological landscape [26]. Additionally, Momtaz *et al.* noted prolonged recovery from inactivation of the high-threshold calcium current in hypertrophic cells, contributing to the overall electrophysiological remodelling [24].

Linking structural remodelling and electrophysiological changes

To connect ECG changes with myocardial remodelling, we analysed correlations between structural and ECG parameters. The near-significant correlation between QRS width and MFV suggests a possible relationship between ventricular depolarization changes and myocardial hypertrophy. However, other ECG parameters did not correlate with the structural changes observed on MRI. This may be due to the fact that MRI primarily focuses on ventricular structures, while detailed imaging of the atria is challenging due to their

small size, position, and the technical limitations of the used setup. Therefore, ECG parameters like the P wave and PR interval lack corresponding structural correlates in the MRI findings.

Study Limitations

This study has some limitations. ECG parameters can be influenced by various experimental conditions, such as anaesthesia, age, and the body mass/size of the animals. Ketamine/xylazine anaesthesia was used, to which some animals exhibited lower responsiveness. Isoflurane, considered a safer anaesthetic agent, might be a better alternative in future studies [27]. Changes in plasma ion levels, such as sodium and potassium, may be expected in the DOCA/salt model and could potentially contribute to the observed ECG alterations. Nevertheless, we did not analyse plasma ion concentrations in this study. Future studies should include biochemical analysis to further investigate this relationship. The averaging method used for ECG analysis may alter the ECG curve and reduce sensitivity. Implementing advanced ECG pre-processing and analysis techniques might improve the accuracy of analyses [28]. Fibrotic tissue may attenuate ECG voltage, diminishing the sensitivity of ECG measurements for detecting left ventricular hypertrophy [29]. Additionally, previously discussed limitations of MRI in small-animal heart imaging further impact the study [14]. A limitation of our study is the lack of focus on sex differences, as only male rats were included. Previous research has shown that sex differences can influence the blood pressure increase in the DOCA/salt model [30]. Future studies should therefore include both male and female subjects to better understand how these differences may affect the outcomes of myocardial remodelling and related electrophysiological changes.

Conclusions

This study demonstrates that significant myocardial remodelling occurs within a short period of just three weeks in the rat DOCA/salt model, characterized by increased left ventricular wall thickness, increased myocardial fractional volume, and the development of myocardial fibrosis. Despite these changes, the left ventricular ejection fraction remains preserved at this stage. This study is among the first to show that early myocardial remodelling in this model is

accompanied by distinct electrophysiological changes, as evidenced by PR interval prolongation and QRS complex widening, indicating altered atrioventricular and ventricular conduction. These findings highlight the rapid onset of both structural and electrophysiological alterations following nephrectomy and DOCA/salt intervention. The rat DOCA/salt model thus provides a valuable platform for investigating the early stages of myocardial remodelling and its impact on cardiac electrophysiology. Furthermore, combining advanced techniques with established animal models creates new opportunities for research in myocardial remodelling.

Conflict of Interest

There is no conflict of interest.

References

1. Mills KT, Stefanescu A, He J. The global epidemiology of hypertension. *Nat Rev Nephrol* 2020;16:223-237. <https://doi.org/10.1038/s41581-019-0244-2>
2. Dictionary M.-W. c. s.v. "hypertension". <https://www.merriam-webster.com/dictionary/hypertension> (accessed 2024 25. January).
3. Lenfant C, Chobanian A, Jones D, Roccella E. Seventh report of the Joint National Committee on the prevention, detection, evaluation, and treatment of high blood pressure (JNC 7) resetting the hypertension sails. *Hypertension* 2003;41:1178-1179. <https://doi.org/10.1161/01.HYP.0000075790.33892.AE>
4. Azevedo PS, Polegato BF, Minicucci MF, Paiva SAR, Zornoff LAM. Cardiac Remodeling: Concepts, Clinical Impact, Pathophysiological Mechanisms and Pharmacologic Treatment. *Arq Bras Cardiol* 2016;106:62-69. <https://doi.org/10.5935/abc.20160005>
5. Tsuda T. Clinical Assessment of Ventricular Wall Stress in Understanding Compensatory Hypertrophic Response and Maladaptive Ventricular Remodeling. *J Cardiovasc Dev Dis* 2021;8:122. <https://doi.org/10.3390/jcdd8100122>
6. Laska M, Nováková M, Stracina T. Myocardium Remodelling: From Adaptation Mechanisms to Heart Failure Development. *Cor Vasa* 2024;66:53-64. <https://doi.org/10.33678/cor.2023.090>
7. Wang Y, Wang M, Samuel CS, Widdop RE. Preclinical rodent models of cardiac fibrosis. *Br J Pharmacol* 2022;179:882-899. <https://doi.org/10.1111/bph.15450>
8. Conrad CH, Brooks WW, Hayes JA, Sen S, Robinson KG, Bing OHL. Myocardial fibrosis and stiffness with hypertrophy and heart failure in the spontaneously hypertensive rat. *Circulation* 1995;91:161-170. <https://doi.org/10.1161/01.CIR.91.1.161>
9. Qi GM, Jia LX, Li YL, Bian YF, Cheng JZ, Li HH, Xiao CS, Du J. Angiotensin II Infusion-Induced Inflammation, Monocytic Fibroblast Precursor Infiltration, and Cardiac Fibrosis are Pressure Dependent. *Cardiovasc Toxicol* 2011;11:157-167. <https://doi.org/10.1007/s12012-011-9109-z>
10. Kobayashi N, Hara K, Watanabe S, Higashi T, Matsuoka H. Effect of imidapril on myocardial remodeling in L-NAME-induced hypertensive rats is associated with gene expression of NOS and ACE mRNA. *Am J Hypertens* 2000;13:199-207. [https://doi.org/10.1016/S0895-7061\(99\)00117-X](https://doi.org/10.1016/S0895-7061(99)00117-X)
11. Farag A, Mandour AS, Hendawy H, Elhaieg A, Elfadadny A, Tanaka R. A review on experimental surgical models and anesthetic protocols of heart failure in rats. *Front Vet Sci* 2023;10:1103229. <https://doi.org/10.3389/fvets.2023.1103229>
12. Zhou H, Chen X, Chen LZ, Zhou X, Zheng GS, Zhang HQ, Huang WJ, Cai JJ. Anti-Fibrosis Effect of Scutellarin via Inhibition of Endothelial-Mesenchymal Transition on Isoprenaline-Induced Myocardial Fibrosis in Rats. *Molecules* 2014;19:15611-15623. <https://doi.org/10.3390/molecules191015611>

Acknowledgements

The study was funded by Masaryk University as a part of the projects no. MUNI/A/1343/2022, MUNI/A/1547/2023, and MUNI/A/1559/2023 with the support of the Specific University Research Grant, as provided by the Ministry of Education, Youth and Sports of the Czech Republic (MEYS CR) in the years 2023 and 2024. The co-operation with the Institute of Scientific Instruments of the Czech Academy of Sciences was supported by the Czech Science Foundation grant (GA22-10953S), all MR experiments were carried out at the ISI-MR facility of the Czech-BioImaging infrastructure, supported by grant LM2023050 of the MEYS CR. We would like to thank the Animal centre ICRC for lending us the equipment used in our research.

13. Basting T, Lazartigues E. DOCA-Salt Hypertension: an Update. *Curr Hypertens Rep* 2017;19:32. <https://doi.org/10.1007/s11906-017-0731-4>
14. Vitous J, Jirík R, Stracina T, Hendrych M, Nádenícek J, Macícek O, Tian Y, ET AL. T1 mapping of myocardium in rats using self-gated golden-angle acquisition. *Magn Reson Med* 2024;91:368-380. <https://doi.org/10.1002/mrm.29846>
15. Bankhead P, Loughrey MB, Fernandez JA, Dombrowski Y, McArt DG, Dunne PD, McQuaid S, ET AL. QuPath: Open source software for digital pathology image analysis. *Sci Rep* 2017;7:16878. <https://doi.org/10.1038/s41598-017-17204-5>
16. Sun ZJ, Zhang ZE. Historic perspectives and recent advances in major animal models of hypertension. *Acta Pharmacol Sin* 2005;26:295-301. <https://doi.org/10.1111/j.1745-7254.2005.00054.x>
17. O'Donaughy TL, Brooks VL. Deoxycorticosterone acetate-salt rats - Hypertension and sympathoexcitation driven by increased NaCl levels. *Hypertension* 2006;47:680-685. <https://doi.org/10.1161/01.HYP.0000214362.18612.6e>
18. Gutkind JS, Kurihara M, Saavedra JM. Increased angiotensin-II receptors in brain nuclei of DOCA-salt hypertensive rats. *Am J Physiol* 1988;255:H646-H650. <https://doi.org/10.1152/ajpheart.1988.255.3.H646>
19. Brown L, Duce B, Miric G, Sernia C. Reversal of cardiac fibrosis in deoxycorticosterone acetate salt hypertensive rats by inhibition of the renin-angiotensin system. *J Am Soc Nephrol* 1999;10(Suppl 11):S143-S148.
20. Grobe JL, Mecca AP, Mao HY, Katovich MJ. Chronic angiotensin-(1-7) prevents cardiac fibrosis in DOCA-salt model of hypertension. *Am J Physiol Heart Circ Physiol* 2006;290:H2417-H2423. <https://doi.org/10.1152/ajpheart.01170.2005>
21. Lovelock JD, Monasky MM, Jeong EM, Lardin HA, Liu H, Patel BG, Taglieri DM, ET AL. Ranolazine Improves Cardiac Diastolic Dysfunction Through Modulation of Myofilament Calcium Sensitivity. *Circ Res* 2012;110:841-850. <https://doi.org/10.1161/CIRCRESAHA.111.258251>
22. Joukar S. A comparative review on heart ion channels, action potentials and electrocardiogram in rodents and human: extrapolation of experimental insights to clinic. *Lab Anim Res* 2021;37:25. <https://doi.org/10.1186/s42826-021-00102-3>
23. Frangogiannis NG. Cardiac fibrosis: Cell biological mechanisms, molecular pathways and therapeutic opportunities. *Mol Aspects Med* 2019;65:70-99. <https://doi.org/10.1016/j.mam.2018.07.001>
24. Momtaz A, Coulombe A, Richer P, Mercadier JJ, Corabœuf E. Action potential and plateau ionic currents in moderately and severely DOCA-salt hypertrophied rat hearts. *J Mol Cell Cardiol* 1996;28:2511-2522. <https://doi.org/10.1006/jmcc.1996.0243>
25. Capuano V, Ruchon Y, Antoine S, Sant MC, Renaud JF. Ventricular hypertrophy induced by mineralocorticoid treatment or aortic stenosis differentially regulates the expression of cardiac K⁺ channels in the rat. *Mol Cell Biochem* 2002;237:1-10. <https://doi.org/10.1023/A:1016518920693>
26. Coulombe A, Momtaz A, Richer P, Swynghedauw B, Corabœuf E. Reduction of calcium-dependent transient outward potassium current-density in DOCA salt hypertrophied rat ventricular myocytes. *Pflugers Arch* 1994;427:47-55. <https://doi.org/10.1007/BF00585941>
27. Botelho AFM, Joviano-Santos JV, Santos-Miranda A, Menezes-Filho JER, Soto-Blanco B, Cruz JS, Guatimosim C, Melo MM. Non-invasive ECG recording and QT interval correction assessment in anesthetized rats and mice. *Pesq Vet Bras* 2019;39:409-415. <https://doi.org/10.1590/1678-6160-pvb-6029>
28. Stracina T, Ronzhina M, Redina R, Novakova M. Golden Standard or Obsolete Method? Review of ECG Applications in Clinical and Experimental Context. *Front Physiol* 2022;13:867033. <https://doi.org/10.3389/fphys.2022.867033>
29. Dohy Z, Verecke A, Horvath V, Czimbalmos C, Szabo L, Toth A, Suhai FI, ET AL. How are ECG parameters related to cardiac magnetic resonance images? Electrocardiographic predictors of left ventricular hypertrophy and myocardial fibrosis in hypertrophic cardiomyopathy. *Ann Noninvasive Electrocardiol* 2020;25:e12763. <https://doi.org/10.1111/anec.12763>
30. Kawanishi H, Hasegawa Y, Nakano D, Ohkita M, Takaoka M, Ohno Y, Matsumura Y. Involvement of the endothelin ETB receptor in gender differences in deoxycorticosterone acetate-salt-induced hypertension. *Clin Exp Pharmacol Physiol* 2007;34:280-285. <https://doi.org/10.1111/j.1440-1681.2007.04580.x>